WIR. COMM. AND MOBI. COMPU.
Wirel. Commun. Mob. Comput. **00**: 1–16 (0000)
Posted online
(wiley inter science) DOI: 10.1002/wcm.0000

Adaptive Low-Energy Clustering In Slotted Beacon-Enabled IEEE 802.15.4 Networks

Hamidreza Tavakoli[1], Jelena Mišić[2], Majid Naderi[3] and Vojislav B. Mišić[2]

[1]*Hakim Sabzevari University, Sabzevar, Iran*
[2]*Ryerson University, Toronto, ON, Canada*
[3]*Iran University of Science and Technology, Tehran, Iran*

Summary

We present, model, and evaluate a novel clustering algorithm running on top of IEEE 802.15.4 wireless sensor networks operating in slotted, beacon-enabled mode. The Adaptive Low-Energy Clustering (ALEC) algorithm provides randomized sleep and randomized rotation of the cluster-head role so as to maximize the useful lifetime of the network by improving efficiency and balancing the lifetime of individual nodes. We model the ALEC algorithm through probabilistic analysis and show that its parameters can be tuned to extend the network lifetime and reduce the delay and energy overhead imposed by clustering. Copyright © 0000 copyright owner, Ltd.

KEY WORDS: Wireless sensor networks; IEEE 802.15.4; clustering; randomized sleeping; rotation of cluster-head role; energy efficiency

1. Introduction

Wireless sensor networks used for data collection in industry, healthcare, and other areas are often implemented using IEEE 802.15.4, a recent network communication technology [12]. In many applications where WSNs operate on battery power, battery replacement is costly or even impossible, and extending the lifetime of the nodes and, consequently, the network itself is one of the most important goals in WSN design [15, 27, 26]. Extending node lifetime is achieved by minimizing the energy consumption for each node individually, but also by ensuring balanced energy consumption of all the nodes in the network [17]. The latter is often achieved by clustering, a procedure whereby the nodes are divided into groups [3, 4], as shown in Fig. 1, in order to obtain the following benefits:

- By reducing the number of direct communications with the base station, reduced transmission power can be used for intra-cluster communication and the number of collisions is considerably reduced. As the result, substantial energy savings and lifetime extension can be achieved, while latency is reduced [16].
- Under contention-based Medium Access Control (MAC) algorithms, dividing the network into clusters reduces the number of contending nodes [31] which lowers the probability of collisions during medium access and improves both bandwidth utilization and energy efficiency.
- Finally, routing overhead may be reduced through clustering as the routing tables need not be updated as often [4].

In each group or cluster, one of the nodes is chosen as a leader or Cluster-Head (CH). A CH node collects the sensing data from individual nodes in its cluster and delivers it to the base station (BS). Since this functionality results in higher energy consumption for CH nodes, they are likely to die

LaTeX'ed with wcmauthX.cls *[Version: 2007/01/09 v1.00]*

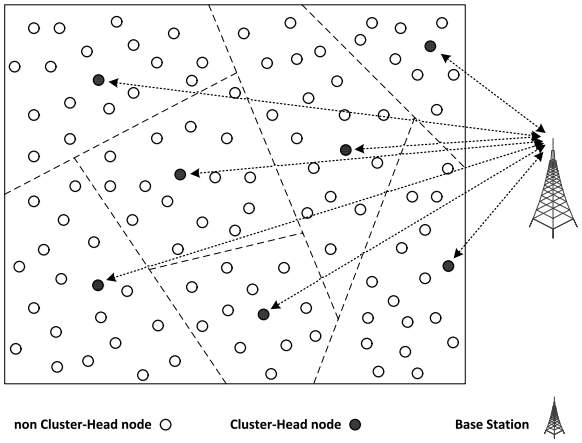

Fig. 1. Topology of the network for round i.

earlier. To reduce this imbalance, the CH role has to be periodically reassigned to different nodes in the cluster so that most, if not all, nodes act in that role for a certain period of time, which may be a constant or random value that follows a predefined probability distribution. However, the manner in which the CH role is assigned to individual nodes must be carefully designed in order to maintain the desirable features such as low data latency and coverage.

In this paper, we describe, analyze, and evaluate a novel clustering algorithm referred to as Adaptive Low-Energy Clustering (ALEC). ALEC is based on probabilistic sleep of individual nodes and probabilistic rotation of the CH role through a simple and efficient distributed election, specifically tailored for use in IEEE 802.15.4 beacon-enabled networks. As far as we know, this is one of the first proposals that includes both probabilistic sleep and probabilistic rotation of the CH role, and the first to present a comprehensive analytical treatment of the impact of clustering on node and network lifetime that incorporates realistic models for node operation at both MAC and physical (PHY) layers. Using these models, we evaluate the performance of a WSN that uses ALEC, and show the impact of various network and ALEC parameters. We also discuss the choice of parameters to ensure balanced power consumption in order to help prolong network lifetime.

The remainder of the paper is organized as follows. Section 2 reviews most relevant results from the literature. Section 3 describes the ALEC algorithm. Sections 4 and 5 present the analytical model for energy consumption of ALEC algorithm. Section 6 evaluates ALEC algorithm's performance and discusses the results. Summary and some directions for future research are given in Section 7.

2. Related work

Clustering has been shown to increase scalability and lifetime of wireless sensor networks [6]. Depending on the manner in which the CH role is assigned to individual nodes, we distinguish between distributed and centralized methods. Distributed approaches typically use probabilistic methods in which selection of CH nodes is based on various criteria such as the number of clusters, age of CHs [9], residual energy of nodes [8], amount of traffic, number of neighbors [2], and density of sensor nodes [20]. However, distributed approaches suffer from the fact that individual sensor nodes do not possess complete knowledge of the network - the only such node is the BS, which has more energy and higher processing power than ordinary nodes. However, centralized elections necessitate periodic exchange of status information between BS and sensor nodes [10] which may lead to extra power consumption [28]. Furthermore, CH selection and clustering may interfere with data communications and thus lead to excessive delay overhead [3].

We note that CH election is often linked to re-clustering, i.e., re-distribution of nodes into clusters, which imposes additional power consumption as well as delay overhead, since the transmission of sensing data is reduced or completely suspended during this process [20]. To reduce communication costs, [14] reinforces clustering only among nodes in close proximity to each other. Alternatively, an energy threshold may be introduced so that only the CHs with lower energy level are allowed to take part in the election, while others retain their role during the following round [11].

Regarding analysis of WSNs with clustering, probabilistic analysis is often used to model event-based and query-based applications in order to determine clustering efficiency and lifetime of the network. Assuming fixed shapes for clusters, authors in [21], derive the probability of achieving a desired cluster lifetime under random assignment of nodes to clusters.

Proposed MAC protocols for sensor networks provide either contention-based access, usually through some form of CSMA-CA, or time division multiple access (TDMA) [5]. The latter offer better power efficiency since individual nodes can enter inactive state until their allocated time slots [5], and they also

DOI: 10.1002/wcm

eliminate packet re-transmissions caused by packet collisions. However, designing a collision-free TDMA schedule with minimum number of time slots and maximum slot usage is an NP-complete problem [5, 13, 24], even without accounting for the need to synchronize the nodes [3].

In comparison to TDMA protocols, contention-based MAC protocols are scalable, more efficient, and easier to implement. One of the most widely used technologies with a contention-based MAC is the IEEE 802.15.4 standard [12] that is specifically tailored towards networks with raw data rate below 250kbps. Therefore, we have chosen this technology as the foundation for our clustering protocol.

3. Adaptive Low-Energy Clustering: ALEC

We assume that all clusters operate in beacon-enabled, slotted CSMA-CA mode, with their CHs acting as coordinators. Additionally, CHs form a separate cluster under the control of the BS. For all clusters, the time is divided into intervals determined by beacons transmitted by CH nodes [12]; the time interval between two successive beacons is referred to as beacon interval $BI = 48 \cdot 2^{BO}$ unit backoff periods, while the duration of an active interval of a superframe is $SD = 48 \cdot 2^{SO}$ unit backoff periods. The variables BO and SO denote the so-called beacon order and superframe order, respectively; their values are chosen so that $0 \leq SO \leq BO \leq 15$. If the operating frequency of the network is 2.4GHz, the interval known as a unit backoff period, is 320μs which translates into 10 bytes and results in raw data rate of 250Kbps. Both uplink and downlink communications use CSMA-CA method at backoff boundaries. However, downlink communications can take place only after announcement of a packet by CH node and downlink request by the corresponding non-CH node [18].

In the inactive part of a superframe, non-CH nodes sleep to reduce energy consumption while CH nodes synchronize to the BS superframe in order to deliver data. As soon as a CH node delivers its data to the BS, it returns to its own cluster and resumes the CH role by sending the beacon frame. If the CH node doesn't succeed in delivering the data to BS in one superframe, it will freeze its backoff counter until the next communication to BS, much like ordinary nodes that do not succeed in sending their data to the respective CHs.

Activity management by adjusting frequency and ratio of active and inactive intervals of sensor nodes is used to reduce energy consumption [23, 25]. Event sensing reliability R, i.e., the number of packets should be received by BS in a suitable time unit, is periodically announced by BS, together with the current number of nodes alive N. Then, each CH node calculates the portion of reliability for its own cluster as $R_k = R(N_k/N)$, where N_k is the number of nodes in cluster k, and broadcasts it to the nodes in its cluster. Using this information, ordinary nodes calculate mean sleep period between transmission attempts; individual sleep periods are calculated randomly in order to reduce collisions [17].

If a node wakes up with a packet in its buffer, it turns its radio on in order to synchronize with the beacon. After finding the beacon, the node transmits the packet and goes back to sleep. If a node wakes up and finds its buffer empty, it will immediately begin a new sleep period. We refer to the sequence of sleep time, beacon finding and packet transmission as a microcycle, as shown in Fig. 2.

After N_μ microcycles, CH nodes are due for re-election. Each node i generates a random number in the range 0 to 1 and compares it with a threshold; if the value is below the threshold, the node becomes a new CH. The threshold depends on the index of the election as

$$T(i,r) = \begin{cases} \dfrac{N_c}{N - N_c(r \bmod \frac{N}{N_c})}, & i \in G \\ 0, & \text{otherwise} \end{cases} \quad (1)$$

where N_c is the desired number of CHs, and G is the set of nodes that were not CHs in the previous $r \mod N/N_c$ elections. In this manner, the number of nodes that compete for election is kept small (ideally, it should be equal to the number of clusters) which minimizes the duration of the re-election interval during which data transmission does not take place.

The time interval during which a given node acts as the CH is referred to as a round. As shown in Fig. 3, each round is composed of a set-up phase, in which CH elections are held and clusters are formed, and a steady-state phase, in which data transmissions are carried out. Each steady-state phase is composed of N_μ packet transmissions, and its duration is referred to as clustering period.

If all intra-cluster communications in the steady-state phase were to occur at the same channel, inter-cluster interference may result. As the IEEE 802.15.4 standard operating in the 2.4GHz ISM band allows the use of 16 channels, inter-cluster interference can be reduced through channel assignment [22]. Still,

DOI: 10.1002/wcm

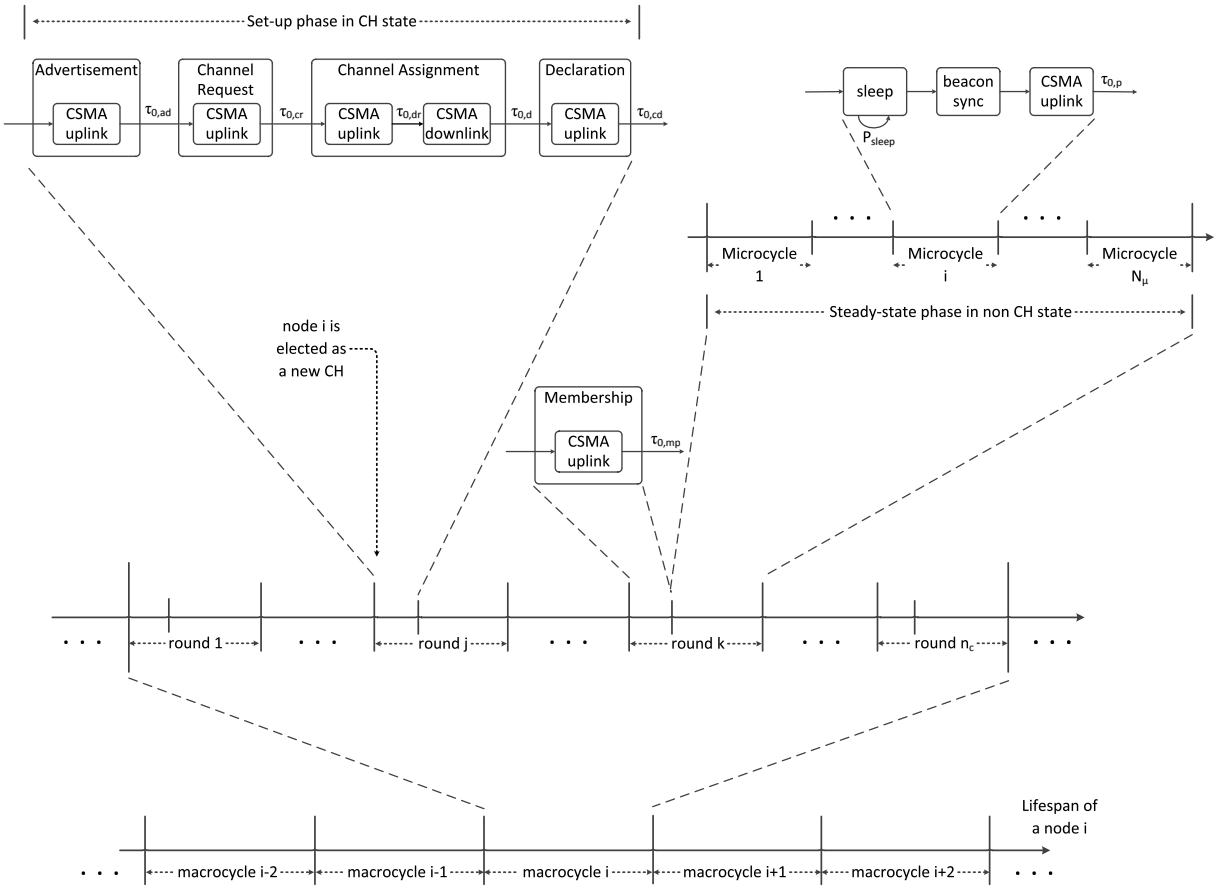

Fig. 2. Pertaining to the operation of ALEC.

communications in the set-up phase must occur on a single channel, the most suitable being channel 26 which is the only one that is free from interference from 802.11 (WiFi) networks [30]. (Channel 26 will also be used by the BS-controlled cluster for data communications during the steady-state phase.)

The set-up phase contains the following activities.

1. Advertisement: after electing as a CH, a node broadcasts its status to other nodes.
2. Membership: each non-CH node determines the CH that requires the minimum transmission power (usually the closest one) and sends it a join request.
3. Channel Request: all CHs inform the BS about the membership of their respective clusters, by sending their IDs along with other IDs they received in membership phase to the BS.
4. Channel Assignment: the BS allocates frequency channels to individual clusters and informs the newly elected CHs accordingly.
5. Channel Declaration: each CH node informs its cluster members about the allocated channel.

The time interval of $n_c = N/N_c$ rounds – which is, in fact, the period of the function used to determine the threshold in r-th election, eq. (1) – will be referred to as a macrocycle. As shown in Fig. 2, a node undergoes a number of macrocycles during its lifetime, and acts as a CH for exactly one round in each macrocycle.

Unlike other clustering algorithms, ALEC introduces randomness at different levels: first, the time interval between successive intervals of CH duty is random due to the election process; and second, the duration of CH duty is random due to the random sleep time of ordinary nodes, random time to transmit the packet due to CSMA-CA backoff time, and possibility of packet collision and packet corruption due to noise.

DOI: 10.1002/wcm

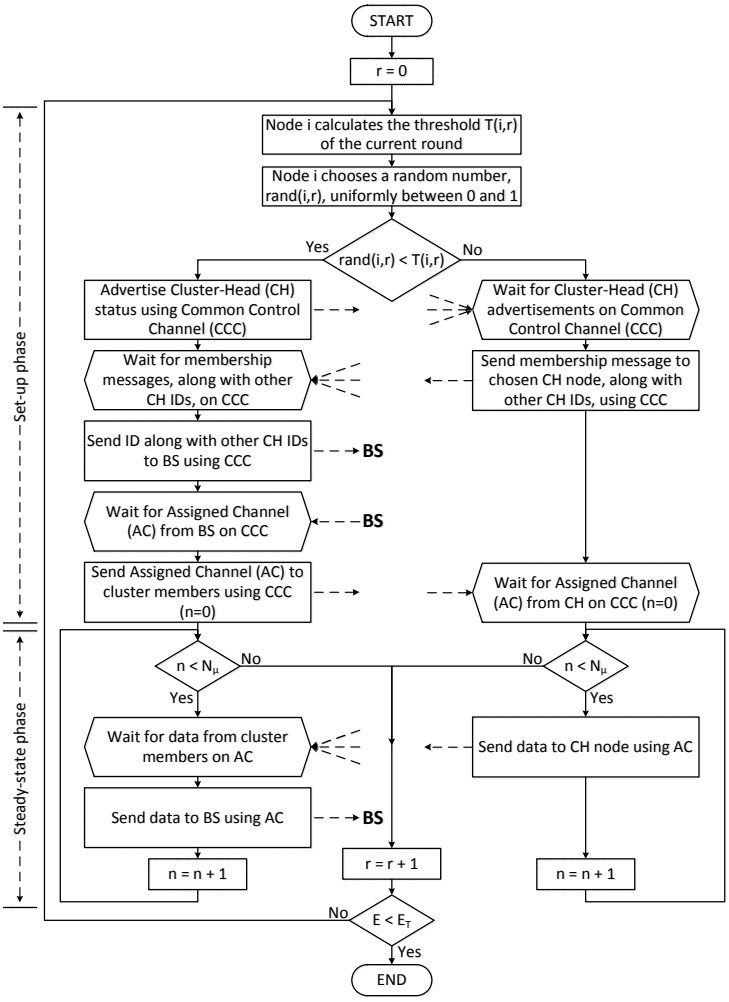

Fig. 3. Flowchart of node operation under ALEC.

4. Modeling ALEC Clustering

Let us now investigate the performance of the ALEC algorithm. We will model activities of individual nodes in the network using Discrete Time Markov Chain (DTMC) with a hierarchical structure. As explained above, a microcycle contains one or more random sleeps with mean duration determined from the event sensing reliability in the cluster, followed by packet transmission. The sequence of microcycles spent in a cluster under a given CH coordination is denoted as a round. In each round, each node will transmit exactly N_μ packets after the set-up phase. A sequence of n_c rounds comprises a macrocycle. We note that the transition between successive macrocycles occurs with probability of one, as do the transitions between rounds within a macrocycle and transitions between microcycles within a round. As the result, the DTMC representing these transitions is irreducible, recurrent and aperiodic, and henceforth ergodic and has a stationary distribution. (We assume that the steady-state of DTMC lasts sufficiently long time.)

A Markov chain for one packet transmission is shown in Fig. 4 (adapted from [18]). The transmission of a packet can start after the current beacon or it can start immediately after the next beacon. The later takes place when transmission of a packet cannot be completed during a superframe [12]. The probability of deferring transmission of a packet to the next beacon (shown as block x in Fig. 4) is P_x. The index x uses to discriminate between data packets (p), advertisement packets (ad), membership packets (mp), channel request packets (cr), downlink request

DOI: 10.1002/wcm

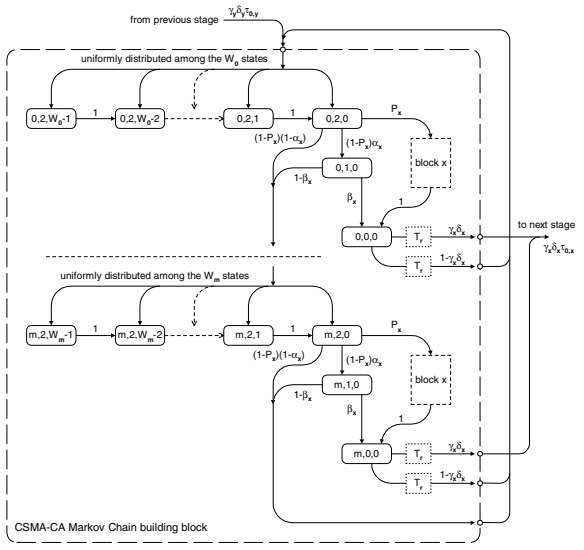

Fig. 4. Markov chain for a packet transmission under CSMA-CA, adapted from [18].

packets (dr), downlink packets (d) and channel declaration packets (cd).

A single packet transmission takes $\overline{D_x} = 2 + \overline{G}_x + 1 + \overline{G}_{ack}$; this time is composed of two Clear Channel Assessments (CCA), the time for actual transmission ($\overline{G_x}$), the time for waiting the acknowledgement (one backoff time in the relation) and the time for transmission of acknowledgement ($\overline{G}_{ack}$). All administrative packets are assumed to last for 3 unit backoff periods and, thus, contain up to 30 bytes which was deemed sufficient. All data packets last for 12 unit backoff periods and, thus, contain up to 120 bytes of data.

Success probabilities for first Clear Channel Assessment, second Clear Channel Assessment and transmission of the packet are labeled as α_x, β_x and γ_x, respectively. The actual transmission, shown with block T_r, is composed of $\overline{D}_x$ backoff durations. The impact of noise and interference is modeled via the probability of a packet being properly received is $\delta_x = 1 - PER = (1 - BER)^{\overline{G}_x + \overline{G}_a}$, where BER denotes bit error rate. We assume to have a reliable MAC layer which mean that the transmission continues until the reception of acknowledgement.

In the Markov chain, a block $\{a, b, c\}$ shows a state of the node in which $a \in \{0 \,..\, m\}$ indicates the number of backoff the node currently spends (m has a constant value of 4); b indicates the number of left Clear Channel Assessments ($b \in \{0, 1, 2\}$); $c \in \{0 \,..\, W_j - 1\}$ indicates the number of backoffs left before Clear Channel Assessments ($W_j = 2^{min(i+macMinBE,5)}$ where *macMinBE* has a constant value of 3). The probability of successfully medium access by a node is denoted as $\tau_{0,x}$.

We will now describe specific features regarding transmission of packets of different types.

4.1. Transmission of packets of different types

Advertisement packets: After the election in the current round, the new CH begins a backoff countdown for the advertisement packet, starting immediately after the beacon. Since the size of first backoff window is between 0 and 7 backoff periods, $P_{ad} = 1/8$ denotes the probability that the chosen backoff time is zero, in which case transmission occurs two backoff periods after the beacon. The total transmission time is, then, $\overline{D_{ad}} = 2 + 3 + 1 = 6$ backoff periods.

During a macrocycle, a node is in advertisement state exactly once. Therefore, the probability of finishing the first backoff phase in the transmission block is

$$x_{0,2,0}^{(ad)} = \frac{\tau_{0,p}\gamma_p\delta_p}{n_c N_\mu} + \tau_{0,ad}(1 - \gamma_{ad}\delta_{ad}). \qquad (2)$$

If we define new variables $C_{1,ad}$, $C_{2,ad}$, $C_{3,ad}$ and $C_{4,ad}$ as

$$\begin{aligned} x_{0,1,0}^{(ad)} &= x_{0,2,0}^{(ad)}(1 - P_{ad})\alpha_{ad} \\ &= x_{0,2,0}^{(ad)} C_{1,ad} \\ x_{1,2,0}^{(ad)} &= x_{0,2,0}^{(ad)}(1 - P_{ad})(1 - \alpha_{ad}\beta_{ad}) \\ &= x_{0,2,0}^{(ad)} C_{2,ad} \\ x_{0,0,0}^{(ad)} &= x_{0,2,0}^{(ad)}((1 - P_{ad})\alpha_{ad}\beta_{ad} + P_{ad}) \\ &= x_{0,2,0}^{(ad)} C_{3,ad} \\ C_{4,ad} &= \frac{1 - C_{2,ad}^{m+1}}{1 - C_{2,ad}} \end{aligned} \qquad (3)$$

the transmission sub-chain can be described with the following:

$$\begin{aligned} x_{i,0,0}^{(ad)} &= x_{0,2,0}^{(ad)} C_{3,ad} C_{2,ad}^i, && i = 0 \,..\, m \\ x_{i,2,k}^{(ad)} &= x_{0,2,0}^{(ad)} \left(1 - \frac{k}{W_i}\right) C_{2,ad}^i \\ & && i = 0 \,..\, m, k = 0 \,..\, W_i - 1 \\ x_{i,1,0}^{(ad)} &= x_{0,2,0}^{(ad)} C_{1,ad} C_{2,ad}^i, && i = 0 \,..\, m \\ x_{0,2,k}^{(ad)} &= x_{0,2,0}^{(ad)} \left(1 - \frac{k}{W_0}\right), k = 0 \,..\, W_0 - 1 \end{aligned} \qquad (4)$$

Access probability for a single advertisement packet is $\tau_{0,ad} = \sum_{i=0}^{m} x_{i,0,0}^{(ad)} = C_{3,ad} C_{4,ad} x_{0,2,0}^{(ad)}$, which can

DOI: 10.1002/wcm

be combined with (2) to obtain

$$\tau_{0,ad} = \frac{C_{3,ad}C_{4,ad}\frac{\tau_{0,p}\gamma_p\delta_p}{n_cN_\mu}}{1 - C_{3,ad}C_{4,ad}(1-\gamma_{ad}\delta_{ad})}. \quad (5)$$

The sum of probabilities for the advertisement packet transmission sub-chain is

$$\begin{aligned} s_{ad} = &\sum_{i=0}^{m}\sum_{k=0}^{W_i-1} x_{i,2,k} \\ &+ (\overline{D}_{ad}-2)\sum_{i=0}^{m} x_{i,0,0} + \sum_{i=0}^{m} x_{i,1,0} \end{aligned} \quad (6)$$

which can be simplified to

$$\begin{aligned} s_{ad} = &x_{0,2,0}^{(ad)} C_{4,ad}\left(C_{3,ad}(\overline{D_{ad}}-2)+C_{1,ad}\right) \\ &+ x_{0,2,0}^{(ad)}\sum_{i=0}^{m}\frac{C_{2,ad}^{i}(W_i+1)}{2} \end{aligned} \quad (7)$$

Membership packets: After the advertisement sub-phase, non-CH nodes start sending membership messages to their CHs. (Note that in a macrocycle, a node acts as an ordinary node in all rounds except the one during which it acts as a CH.) Membership packets, similar to advertisement packets, are sent after the beacon, therefore $P_{mp} = 1/8$.

In the Markov chain, the probability of the first backoff being successful is $x_{0,2,0}^{(mp)} = \frac{(n_c-1)\tau_{0,p}\gamma_p\delta_p}{n_cN_\mu} + \tau_{0,mp}(1-\gamma_{mp}\delta_{mp})$. Following an approach similar to the one outlined above, we get

$$\tau_{0,mp} = \frac{C_{3,mp}C_{4,mp}\frac{(n_c-1)\tau_{0,p}\gamma_p\delta_p}{n_cN_\mu}}{1 - C_{3,mp}C_{4,mp}(1-\gamma_{mp}\delta_{mp})} \quad (8)$$

The sum of probabilities for the transmission of membership packets can, then, be written as

$$\begin{aligned} s_{mp} = &x_{0,2,0}^{(mp)} C_{4,mp}\left(C_{3,mp}(\overline{D_{mp}}-2)+C_{1,mp}\right) \\ &+ x_{0,2,0}^{(mp)}\sum_{i=0}^{m}\frac{C_{2,mp}^{i}(W_i+1)}{2} \end{aligned} \quad (9)$$

Channel request packets: Information on cluster membership gathered during the membership sub phase is sent by the CHs to the BS. Channel request packets start after the beacon, therefore $P_{cr} = 1/8$, and their duration is assumed to be $\overline{G}_{cr} = 3$ backoff periods, as noted above.

In the Markov chain for a channel request packet, the probability of the first backoff being successful is $x_{0,2,0}^{(cr)} = \tau_{0,ad}\gamma_{ad}\delta_{ad} + \tau_{0,cr}(1-\gamma_{cr}\delta_{cr})$. Following an approach similar to the one outlined above for the advertisement packets, we obtain

$$\tau_{0,cr} = \frac{C_{3,cr}C_{4,cr}\gamma_{ad}\delta_{ad}\tau_{0,ad}}{1 - C_{3,cr}C_{4,cr}(1-\gamma_{cr}\delta_{cr})}. \quad (10)$$

The sum of probabilities for transmission of channel request packets can be, then, obtained as

$$\begin{aligned} s_{cr} = &x_{0,2,0}^{(cr)} C_{4,cr}\left(C_{3,cr}(\overline{D_{cr}}-2)+C_{1,cr}\right) \\ &+ x_{0,2,0}^{(cr)}\sum_{i=0}^{m}\frac{C_{2,cr}^{i}(W_i+1)}{2} \end{aligned} \quad (11)$$

Downlink request packets: In order to apply for a downlink request packet, the node starts a backoff attempt in the beginning of the superframe. Downlink request packets start after the beacon with probability of $P_{dr} = 1/8$. Probability that the first backoff is successful for a downlink request packet is $x_{0,2,0}^{(dr)} = \tau_{0,cr}\gamma_{cr}\delta_{cr} + \tau_{0,dr}(1-\gamma_{dr}\delta_{dr})$, and the corresponding access probability is

$$\tau_{0,dr} = \frac{C_{3,dr}C_{4,dr}\gamma_{cr}\delta_{cr}\tau_{0,cr}}{1 - C_{3,dr}C_{4,dr}(1-\gamma_{dr}\delta_{dr})}. \quad (12)$$

The sum of probabilities for the transmission of request packets can be, then, obtained as

$$\begin{aligned} s_{dr} = &x_{0,2,0}^{(dr)} C_{4,dr}\left(C_{3,dr}(\overline{D_{dr}}-2)+C_{1,dr}\right) \\ &+ x_{0,2,0}^{(dr)}\sum_{i=0}^{m}\frac{C_{2,dr}^{i}(W_i+1)}{2} \end{aligned} \quad (13)$$

Downlink packets with channel assignment information: Downlink packets can be transmitted only upon successful acknowledgment of downlink request packets. Probability that a packet will be delayed is $P_d = \overline{D_d}/SD$, where SD denotes the active superframe duration. Probability of finishing the first backoff phase in the transmission block for a downlink packet is $x_{0,2,0}^{(d)} = \tau_{0,dr}\gamma_{dr}\delta_{dr} + \tau_{0,d}(1-\gamma_d\delta_d)$, while the corresponding access probability is

$$\tau_{0,d} = \frac{C_{3,d}C_{4,d}\gamma_{dr}\delta_{dr}\tau_{0,dr}}{1 - C_{3,d}C_{4,d}(1-\gamma_d\delta_d)}. \quad (14)$$

The sum of probabilities for the transmission of downlink packets can be, then, obtained as

$$\begin{aligned} s_d = &\sum_{i=0}^{m}\sum_{k=0}^{W_i-1} x_{i,2,k}^{(d)} + (\overline{D_d}-2)\sum_{i=0}^{m} x_{i,0,0}^{(d)} \\ &+ \sum_{i=0}^{m} x_{i,1,0}^{(d)} + \sum_{i=0}^{m}\sum_{l=0}^{\overline{D}_d-1} x_{i,2,0,l}^{(d)} \end{aligned} \quad (15)$$

DOI: 10.1002/wcm

which can be simplified to

$$s_d = x_{0,2,0}^{(d)} C_{4,d} \mathcal{P}_{dca} + x_{0,2,0}^{(d)} \sum_{i=0}^{m} \frac{C_{2,d}^{i}(W_i+1)}{2} \tag{16}$$

where $\mathcal{P}_{dca} = C_{3,d}(\overline{D_d}-2)+C_{1,d}+P_d(\overline{D_d}-1)/2$.

Channel declaration packets: The transmission of these packets, which follow the downlink packets, begins in the second half of the current superframe or in the beginning of the next superframe, therefore $P_{cd} = \overline{D_{cd}}/SD$. The duration of the channel declaration packet is $\overline{G}_{cd} = 3$ backoff periods.

The probability of a channel declaration packet successfully finishing the first backoff phase in the transmission block is $x_{0,2,0}^{(cd)} = \tau_{0,d}\gamma_d\delta_d + \tau_{0,cd}(1-\gamma_{cd}\delta_{cd})$, while the corresponding access probability is

$$\tau_{0,cd} = \frac{C_{3,cd}C_{4,cd}\gamma_d\delta_d\tau_{0,d}}{1-C_{3,cd}C_{4,cd}(1-\gamma_{cd}\delta_{cd})} \tag{17}$$

and the sum of probabilities for the corresponding sub-chain is

$$s_{cd} = x_{0,2,0}^{(cd)} C_{4,cd} \mathcal{P}_{cd} + x_{0,2,0}^{(cd)} \sum_{i=0}^{m} \frac{C_{2,cd}^{i}(W_i+1)}{2} \tag{18}$$

where, similar to the case of downlink packets with channel assignment information, $\mathcal{P}_{cd} = C_{3,cd}(\overline{D_{cd}}-2)+C_{1,cd}+P_{cd}(\overline{D_{cd}}-1)/2$.

Data packets: A node that wakes up and finds a packet in its buffer will wait for the beacon to synchronize and begin its backoff countdown in order to send the packet to its CH. We denote $P_p = 1/8$ as the probability of occurring transmission in the beginning of the superframe because the first window for backoff attempt is 8. In this case, the CCAs will be successful. The length of data packets is $\overline{D_p} = 12$ backoff periods, as noted above.

In the Markov chain for a data packet, the probability that the first backoff is finished is

$$x_{0,2,0}^{(p)} = \frac{\tau_{0,mp}\gamma_{mp}\delta_{mp} + (N_\mu-1)\tau_{0,p}\gamma_p\delta_p}{N_\mu} + \tau_{0,p}(1-\gamma_p\delta_p), \tag{19}$$

and the corresponding access probability is

$$\tau_{0,p} = \frac{C_{3,p}C_{4,p}\tau_{0,mp}\gamma_{mp}\delta_{mp}/N_\mu}{1-C_{3,p}C_{4,p}\left(\frac{(N_\mu-1)\gamma_p\delta_p}{N_\mu}+(1-\gamma_p\delta_p)\right)}. \tag{20}$$

Sum of total probabilities for the sensing data packet transmission sub-chain is

$$\begin{aligned} s_p = \; & x_{0,2,0}^{(p)} C_{4,p}\left(C_{3,p}(\overline{D_p}-2)+C_{1,p}\right) \\ & + x_{0,2,0}^{(p)} \sum_{i=0}^{m} \frac{C_{2,p}^{i}(W_i+1)}{2} \end{aligned} \tag{21}$$

Synchronization times: Synchronization time is the time interval between wake-up time and the subsequent cluster beacon, for an ordinary node, or the time interval between switching to the BS cluster and the subsequent BS cluster beacon, for a CH node. Since the distribution of synchronization period is uniform, the Probability Generating Function (PGF) can be determined as $D(z) = \frac{1-z^{BI}}{BI(1-z)}$. Sum of total probabilities within the beacon synchronization time during steady-state phase is

$$s_{ss} = \frac{\tau_{0,mp}\gamma_{mp}\delta_{mp}+(N_\mu-1)\tau_{0,p}\gamma_p\delta_p}{N_\mu} \sum_{i=0}^{BI} \frac{i}{BI} \tag{22}$$

The probability distribution of sleep period of a node is geometric with the average value of $frac1P_{sleep}$ [17]. Sum of total probabilities that a node spends in a single sleep period is

$$s_{s1} = \frac{\tau_{0,mp}\gamma_{mp}\delta_{mp} + (N_\mu-1)\tau_{0,p}\gamma_p\delta_p}{N_\mu(1-P_{sleep})}. \tag{23}$$

As noted above, when a node wakes up, it checks if there is a packet in its buffer and if so, it will attempt to send it. The probability of the event is denoted as P_c and the value will be determined later. Sum of total probabilities that a node spends in a sleep cycle is $s_s = \frac{s_{s1}}{(1-P_c)}$.

The normalization condition for the complete Markov chain is

$$\begin{aligned} & (n_c-1)(s_{ss}+N_\mu(s_s+s_{ss}+s_p))+ \\ & s_{ad}+s_{cr}+s_{dr}+s_d+s_{cd} = 1 \end{aligned} \tag{24}$$

For a specific packet type, total access probability can be determined as sum of the access probabilities in a macrocycle, taking into account that some of activities actually occur only once per round:

$$\begin{aligned} \tau_p &= (n_c-1)N_\mu\tau_{0,p} \\ \tau_{mp} &= (n_c-1)\tau_{0,mp} \\ \tau_{ad} &= \tau_{0,ad} \\ \tau_{cr} &= \tau_{0,cr} \\ \tau_{dr} &= \tau_{0,dr} \\ \tau_d &= \tau_{0,d} \\ \tau_{cd} &= \tau_{0,cd} \end{aligned} \tag{25}$$

DOI: 10.1002/wcm

The analysis of the transmission of data packets and synchronization times in the last two sub-subsections above applies to both data transmissions from a sensing node to its CH in an individual cluster, and to data transmissions from a CH to the BS in the BS cluster.

4.2. Analysis of the packet queue at the node

MAC layer will be modeled as an $M/G/1/K$ queue with the following Markov points: sleep period, beacon synchronization, cluster set-up and service time of the packet. Packet arrivals to the queue of a node follow the Poisson process with average arrival rate of λ. The buffer of nodes has the capacity of L packets. The node that has packets will send a single packet before going to sleep, which is known as 1-limited scheduling policy [29]. The PGF of the duration of packet service time is denoted as $T_{t,x}(z)$, where $x \in \{ad, mp, cr, dr, d, cd, p\}$; the exact value of this PGF will be derived in Section 5. The buffer of a node is modeled using the following Markov points.

Departure time of a data packet: The number of packet arrivals during service time of a packet has the PGF of $B(z) = \sum_{k=0}^{\infty} b_k z^k = T^*_{t,p}(\lambda - z\lambda)$, in which $T^*_{t,p}()$ denotes the Laplace-Stieltjes Transform (LST) of service time [29] and the LST can be obtained by replacing the variable z with e^{-s}. The probability of existing $j \in \{0\,..\,L-1\}$ packets in the node buffer after finishing the service time of a packets is denoted as ν_j.

End of a sleep period: After finishing transmission of a packet (before ending the steady-state phase), the node starts a sleep period. a single sleep period has the PGF of $V(z) = \sum_{j=1}^{\infty}(1-P_{sleep})P_{sleep}^{j-1}z^j = \frac{(1-P_{sleep})z}{1-zP_{sleep}}$. According to [29], during a single sleep period, number of packet arrivals to the buffer of a node has PGF of $E(z) = \sum_{j=0}^{\infty} e_j z^j = V^*(\lambda - z\lambda)$. The probability of existing $j \in \{0\,..\,L\}$ packets in the buffer of a node after finishing a single sleep period is denoted as ω_j.

End of cluster set-up phase: According to Fig. 2, after ending the steady-state phase, the node starts a cluster set-up, during which data packets cannot be transmitted. The set-up state can be assumed as a vacation for the queue of data packet. The PGF of the duration of the set-up is $T_s(z)$ and the number of packets arriving to the buffer during a set-up phase has the PGF of $H(z) = \sum_{j=0}^{\infty} h_j z^j = T^*_s(\lambda - z\lambda)$. The probability of existing $j \in \{0\,..\,L\}$ packets in the buffer of a node after finishing the cluster set-up is denoted as ϵ_j.

End of the synchronization period: After ending of a sleep cycle, the node with a non-empty queue, has to find a beacon. The interval has a uniform distribution between 0 and $BI-1$ backoff, and its PGF $D(z)$ is given in 4.1. During a synchronization period, number of packet arrivals to the buffer of a node has PGF of $F(z) = \sum_{k=0}^{\infty} f_k z^k = D^*(\lambda - z\lambda)$. The probability of existing $j \in \{0\,..\,L\}$ packets in the buffer of a node at the end of synchronization period is denoted as δ_j.

Node buffer behavior in Markov points: By modeling the node buffer state in Markov points of different types, the steady-state equations for state transitions are as follows:

$$
\begin{aligned}
\omega_0 &= (\omega_0 + p\nu_0 + \epsilon_0)e_0, \\
\omega_k &= (\omega_0 + p\nu_0 + \epsilon_0)e_k + \sum_{j=1}^{k} p\nu_j e_{k-j} \\
&\quad + \sum_{j=1}^{k} \epsilon_j e_{k-j}, \qquad 1 \le k \le L-1 \\
\omega_L &= (\omega_0 + p\nu_0 + \epsilon_0) \sum_{k=L}^{\infty} e_k \\
&\quad + \sum_{j=1}^{L-1} p\nu_j \sum_{k=L-j}^{\infty} e_k + \sum_{j=1}^{L-1} \epsilon_j \sum_{k=L-j}^{\infty} e_k \\
\delta_k &= \sum_{j=1}^{k} \omega_j f_{k-j} \qquad 1 \le k \le L-1 \\
\delta_L &= \sum_{j=1}^{k} \omega_j \sum_{k=L-j}^{\infty} f_k \\
\nu_k &= \sum_{j=1}^{k+1} w_j b_{k-j+1}, \qquad 0 \le k \le L-2 \\
\nu_{L-1} &= \sum_{j=1}^{L} w_j \sum_{k=L-j}^{\infty} b_k \\
\epsilon_k &= \sum_{j=0}^{k} (1-p)\nu_j h_{k-j}, 1 \le k \le L-1 \\
\epsilon_L &= \sum_{j=0}^{k} (1-p)\nu_j \sum_{k=L-j}^{\infty} h_k
\end{aligned}
\tag{26}
$$

DOI: 10.1002/wcm

together with the normalization equation

$$\sum_{k=0}^{L}(\omega_k+\epsilon_k)+\sum_{k=1}^{L}\delta_k+\sum_{k=0}^{L-1}\nu_k=1 \qquad (27)$$

where $1-p=1/N_\mu$ denotes the probability of being in the last transmission of the current steady-state phase. After solving the equations, the probability of the queue length at Markov points will be found. Solving the equations results in obtaining the value of $P_c=\omega_0/\sum_{i=0}^{L}\omega_i$. Therefore, mean sleep cycle (which can be composed of a number of sleep periods) is $\overline{I}=1/\left((1-P_c)(1-P_{sleep})\right)$.

4.3. Transmission success probabilities

We assume the packet arrival events follow a Poisson process and there are $n_c=N/N_c$ nodes in a cluster. The traffic generated by all other nodes in a cluster is considered as background traffic for a given node, assuming that the cluster operates below the saturation regime [18].

Arrival rates of packets for background traffic: Since CH nodes are members of the BS cluster, we discriminate between packet arrival rates during their CH and non-CH periods. Transmissions of membership and sensing packets can commence in the first eight backoffs in the beginning of a superframe. The background packet arrival is $\lambda_x=(n_c-1)\tau_x SD/8$, where $x\in\{mp,p\}$.

During CH periods, transmission of advertisement, channel request and downlink request packets can commence in the first eight backoffs in the beginning of a superframe; the arrival rate of background traffic is $\lambda_x=(N_c-1)\tau_x SD/8$, where $x\in\{ad,cr,dr\}$. After a successful reception of a downlink request packet, the transmission of a downlink packet can start. In this case, the arrival rate of background traffic of downlink packets is $\lambda_d=(N_c-1)\tau_d SD/(SD-\overline{D}_{dr})$.

After learning about the assigned channel, the CH node starts transmission of channel declaration packets in the second part of the current superframe or the first part of the immediately following one. The arrival rate of the background traffic can be described by $\lambda_{cd}=(N_c-1)\tau_{cd}$.

The first CCA will fail if any other transmission is in progress while the second CCA will fail if any other transmission has just been started.

Medium behavior: Sensing, advertisement, membership and channel request packets have success probabilities of $\alpha_x=\frac{1}{8}\sum_{i=0}^{7}e^{-i\lambda_x}$, $\beta_x=e^{-\lambda_x}$, and $\gamma_x=\beta_x^{\overline{D_x}}$, respectively, where $x\in\{ad,mp,cr,p\}$.

Downlink request packets have success probabilities of $\alpha_{dr}=\frac{1}{8}\sum_{i=0}^{7}e^{-i(\lambda_{dr}+\lambda_{cd})}$, $\beta_{dr}=e^{-(\lambda_{dr}+\lambda_{cd})}$, and $\gamma_{dr}=\beta_{dr}^{\max(\overline{D_{dr}},\overline{D_{cd}})}$.

Success probabilities for downlink packets are $\alpha_d=\frac{1}{SD-\overline{D}_{dr}}\sum_{i=8}^{SD-\overline{D}_{dr}-1}e^{-i(\lambda_{dr}+\lambda_d+\lambda_{cd})}$, $\beta_d=e^{-(\lambda_{dr}+\lambda_d+\lambda_{cd})}$, and $\gamma_d=\beta_d^{\max(\overline{D}_{dr},\overline{D}_d,\overline{D}_{cd})}$.

Finally, success probabilities for channel declaration packets are $\alpha_{cd}=\frac{1}{SD}\sum_{i=0}^{SD-1}e^{-i(\lambda_{dr}+\lambda_d+\lambda_{cd})}$, $\beta_{cd}=e^{-(\lambda_{dr}+\lambda_d+\lambda_{cd})}$, and $\gamma_{cd}=\beta_{cd}^{\max(\overline{D_{dr}},\overline{D_d},\overline{D_{cd}})}$.

Success probabilities for CH and non-CH nodes: There are N_c clusters containing n_c sensor nodes, each having arrival rate of λ per node. We can assume identical traffic conditions in all clusters during a round.

Before obtaining success probabilities, access probabilities have to be determined. For a specific type of packet, in order to determine access probability, the packet type x should be replaced for τ_x (25).

Access probabilities for packets sent by CHs can be modeled as $\tau_{x,CH}=n_c\tau_x$. As success probability for CH transmissions depends on all other CHs, we arrive at $\gamma_{x,CH}=(1-\tau_{x,CH})^{\overline{D_x}(N_c-1)}$.

5. Analyzing Node Lifetime

For a specific type of packet x with constant length of k_x backoffs, the PGF of length of packet will be assumed as $G_x(z)=z^{k_x}$. We will assume $G_a(z)=z$ is PGF of duration of acknowledgment and $t_{ack}(z)=z^2$ is PGF of duration of intervals between the data and acknowledgment. According to previous assumptions, PGF for duration of a transmission reception of its acknowledgment is $T_x(z)=G_x(z)t_{ack}(z)G_a(z)$. Then, for a specific type of packet x, the PGF of the time interval needed to accomplish transmission of a single packet [18] is

$$\mathcal{A}_x(z)=\frac{\sum_{i=0}^{m}(1-\alpha_x\beta_x)^i z^{2(i+1)}\alpha_x\beta_x T_x(z)\prod_{j=0}^{i}B_j(z)}{\alpha_x\beta_x\sum_{i=0}^{m}(1-\alpha_x\beta_x)^i} \qquad (28)$$

where $B_j(z)=\frac{z^{W_j}-1}{W_j(z-1)}$ is the PGF for the duration of j-th backoff time prior to transmission. The LSTs

DOI: 10.1002/wcm

for energy consumption during wait and reception of acknowledgment, two CCAs and packet transmission are $e^{-3s\omega_r}$, $e^{-2s\omega_r}$, and $e^{-k_x s\omega_t}$, respectively. We assume that the length of beacon necessary for informing the number of live nodes and event sensing reliability is three; hence the LST for energy consumption while receiving it is $e^{-3s\omega_r}$. Then, the LST for energy consumption during transmission of the data packet and reception of acknowledgment will be $T_x^*(s) = e^{-sk_x\omega_t}e^{-s3\omega_r}$. The LST for energy consumption for a single transmission attempt becomes

$$\mathcal{E}^*_{\mathcal{A}x}(s) = \frac{\sum_{i=0}^{m}(1-\alpha_x\beta_x)^i e^{-2s\omega_r(i+1)}\alpha_x\beta_x T_x^*(s)\mathcal{B}}{\alpha_x\beta_x\sum_{i=0}^{m}(1-\alpha_x\beta_x)^i} \tag{29}$$

where $\mathcal{B} = \prod_{j=0}^{i} E^*_{B_j}(s)$.

Considering packet collisions [19], PGF of the total packet service time becomes $T_{t,x}(z) = \sum_{k=0}^{\infty}(\mathcal{A}_x(z)(1-\gamma_x\delta_x))^k\mathcal{A}_x(z)\gamma_x\delta_x$ which can be simplified to $T_{t,x}(z) = \frac{\gamma_x\delta_x\mathcal{A}_x(z)}{1-\mathcal{A}_x(z)+\gamma_x\delta_x\mathcal{A}_x(z)}$, and the LST for the energy spent on a packet service time is $E^*_{T_x}(s) = \frac{\gamma_x\delta_x\mathcal{E}^*_{\mathcal{A}x}(s)}{1-\mathcal{E}^*_{\mathcal{A}x}(s)+\gamma_x\delta_x\mathcal{E}^*_{\mathcal{A}x}(s)}$. Average value of energy consumed for packet transmission is $\overline{E_{Tx}} = -\frac{d}{ds}E^*_{Tx}(s)|_{s=0}$.

CHs send packets during advertisement, channel request, uplink request for channel assignment and channel declaration sub-phases of a given set-up phase; they receive packets during membership sub-phase and sub-phase of downlink data for channel assignment. Non-CH nodes only send packets during membership sub-phase, and they are in receiving mode during other sub-phases of a given set-up phase. Therefore, the PGF of the duration of one set-up phase is $T_s(z) = T_{ad}(z)T_{mp}(z)T_{cr}(z)T_{dr}(z)T_d(z)T_{cd}(z)$ and LST of energy consumption during a single set-up phase is

$$\begin{aligned} E^*_{s,C}(s) &= E^*_{Tad}(s)E^*_{Tcr}(s)E^*_{Tdr}(s)E^*_{Tcd}(s) \\ &\quad \cdot T_{mp}(e^{-s\omega_r})T_d(e^{-s\omega_r}) \\ E^*_{s,nC}(s) &= E^*_{Tmp}(s)T_{ad}(e^{-s\omega_r})T_{cr}(e^{-s\omega_r}) \\ &\quad \cdot T_{dr}(e^{-s\omega_r})T_d(e^{-s\omega_r})T_{cd}(e^{-s\omega_r}) \end{aligned} \tag{30}$$

for CH and non-CH nodes, respectively.

As discussed before, each steady-state phase is composed of a number (N_μ) of microcycles which is composed of three steps: sleep, beacon synchronization and data transmission (CSMA-CA uplink). However, all CH nodes are awake and in receiving mode during a microcycle, therefore the average energy consumption is

$$\begin{aligned} E^*_{m,C}(s) &= I(e^{-s\omega_r})D(e^{-s\omega_r})e^{-s3\omega_r}T_p(e^{-s\omega_r}) \\ E^*_{m,nC}(s) &= I(e^{-s\omega_s})D(e^{-s\omega_r})e^{-s3\omega_r}E^*_{Tp}(s) \end{aligned} \tag{31}$$

for CH and non-CH nodes, respectively.

Then, the LST for energy consumption during a given round is

$$\begin{aligned} E^*_{r,C}(s) &= E^*_{s,C}(s)(E^*_{m,C}(s))^{N_\mu} \\ E^*_{r,nC}(s) &= E^*_{s,nC}(s)(E^*_{m,nC}(s))^{N_\mu} \end{aligned} \tag{32}$$

for CH and non-CH nodes, respectively.

During a macrocycle which is composed of n_c rounds each node has to act as CH for one round only; therefore, the LST for energy consumed during one macrocycle is

$$E^*_M(s) = E^*_{r,C}(s)(E^*_{r,nC}(s))^{n_c-1} \tag{33}$$

If the battery budget is E_{bat}, the average number of macrocycles during lifetime of a node is $E_{bat}/\overline{E_M}$, where $\overline{E_M}$ is the average value of energy consumed during a macrocycle. Therefore, total lifetime of the network is $\overline{L} = \overline{T_M}E_{bat}/\overline{E_M}$, where $\overline{T_M}$ is average duration of a macrocycle.

6. Performance evaluation

To evaluate the performance of the ALEC algorithm, we have solved the system of equations presented in Sections 4 and 5 to obtain relevant performance indicators. We have assume that the network has 400 nodes, each of which is powered by two AA batteries with total energy $E_{bat} = 10260J$. The effect of noise and interference is modeled with $BER = 10^{-4}$. The network operates in the ISM band at 2.4 GHz, with raw data rate of 0.25 Mbps. Superframe and beacon order parameters were set to $SO = 0$ and $BO = 1$, respectively, which means that superframe size was $SD = 48$ unit backoff periods, while the beacon interval was $BI = 96$ backoff periods.

To ensure realistic experimental values, we have assumed that energy consumption per backoff period is $\omega_s = 18.2 \times 10^{-9}J$, $\omega_r = 17.9 \times 10^{-6}J$, and $\omega_t = 15.8 \times 10^{-6}J$, during receiving, sleeping and transmitting at 0 dBm, respectively [1]. Regarding packet length, we note that increasing packet length would result in reduced values for successful transmission and reception rate (γ_x

DOI: 10.1002/wcm

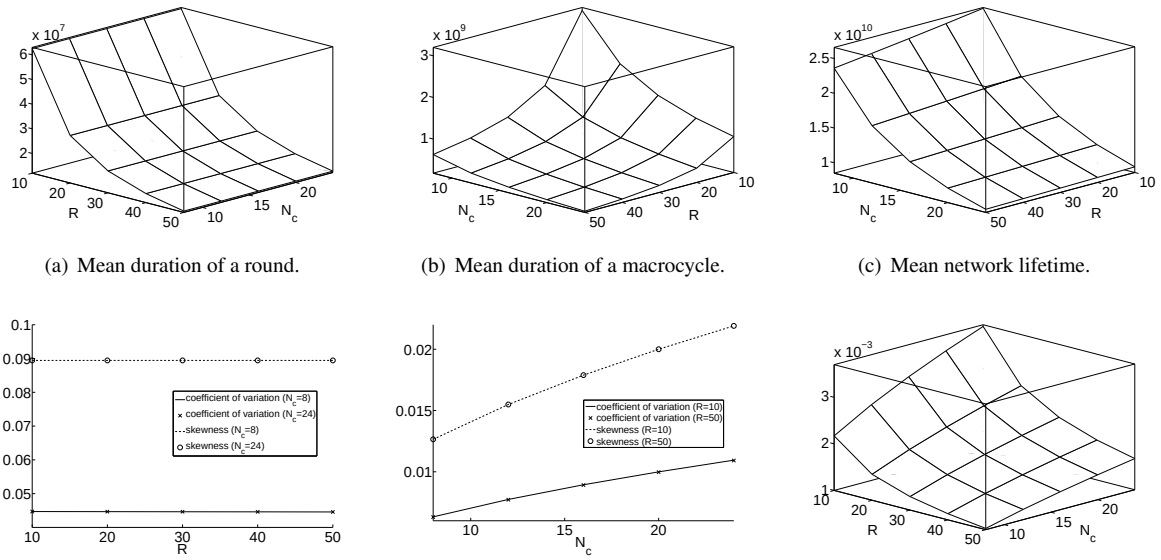

(a) Mean duration of a round. (b) Mean duration of a macrocycle. (c) Mean network lifetime.

(d) Coefficient of variation and skewness of a round. (e) Coefficient of variation and skewness of a macrocycle. (f) Coefficient of variation of lifetime.

Fig. 5. Performance vs. sensing reliability R and number of clusters N_c.

and δ_x, respectively), which translates into more frequent retransmissions and lower energy efficiency. Therefore, we assumed that all packets have the same length of $k_p = 3$ unit backoff periods, except for sensing packets which have the maximum allowed packet length of $k_p = 12$ unit backoff periods. We also assume that each node has a buffer that can hold $L = 2$ packets.

Our main performance indicators will be the mean value of a random variable $\mu = -\frac{d}{ds}F^*(s)|_{s=0}$, where $F^*(s)$ is its LST; the coefficient of variation $CV = \sigma/\mu = \frac{1}{\mu}\left(\frac{d^2}{ds^2}F^*(s)|_{s=0} - \mu^2\right)^{\frac{1}{2}}$, which is a measure of dispersion around the mean; and skewness $\gamma = -\frac{1}{\sigma^3}\left(\frac{d^3}{ds^3}F^*(s)|_{s=0} - 3\mu\sigma^2 - \mu^3\right)$, which is a measure of the degree of asymmetry of a distribution around its mean.

6.1. Variable event sensing reliability and number of clusters

We first investigate performance of ALEC under variable event sensing reliability R (i.e., number of packets per second needed for reliable event detection) and variable number of clusters N_c, while keeping the number of microcycles constant at $N_\mu = 500$. The resulting mean duration of a round, macrocycle, and network lifetime, as well as their coefficient of variation and skewness (except for network lifetime), are shown in Fig. 5. The required event sensing reliability values are obtained by varying the packet arrival rate in the range 0.025 to 0.125 packets per second per node. The average duration of a microcycle is $\overline{T}_m = 1/r = \overline{I} + \overline{D} + 3 + \overline{T}$, from which we can determine the mean inactive period $\overline{I}$ and sleep probability P_{sleep}.

As can be seen in Fig. 5(a), lower values of R lead to higher mean duration of a round. Since a macrocycle is sum of n_c independent and identically distributed (iid) random variables that correspond to individual rounds, mean duration of a macrocycle is the sum of averages of rounds, as in Fig. 5(b). The network lifetime, shown in Fig. 5(c), is also sum of a number of iid random variables representing duration of macrocycles. The coefficient of variation and skewness of a round and a macrocycle are shown in Figs. 5(d) and 5(e), respectively. The variance of the sum of a number of iid random variables is the sum of their variances. Therefore, when the number of random variables to be added increases, the numerator of coefficient of variation (standard deviation) decreases more rapidly than its denominator, which means smaller dispersion around the mean.

When the number of clusters increases, as shown in Fig. 5(e), the number of rounds in a macrocycle decreases, which results in higher dispersion around

DOI: 10.1002/wcm

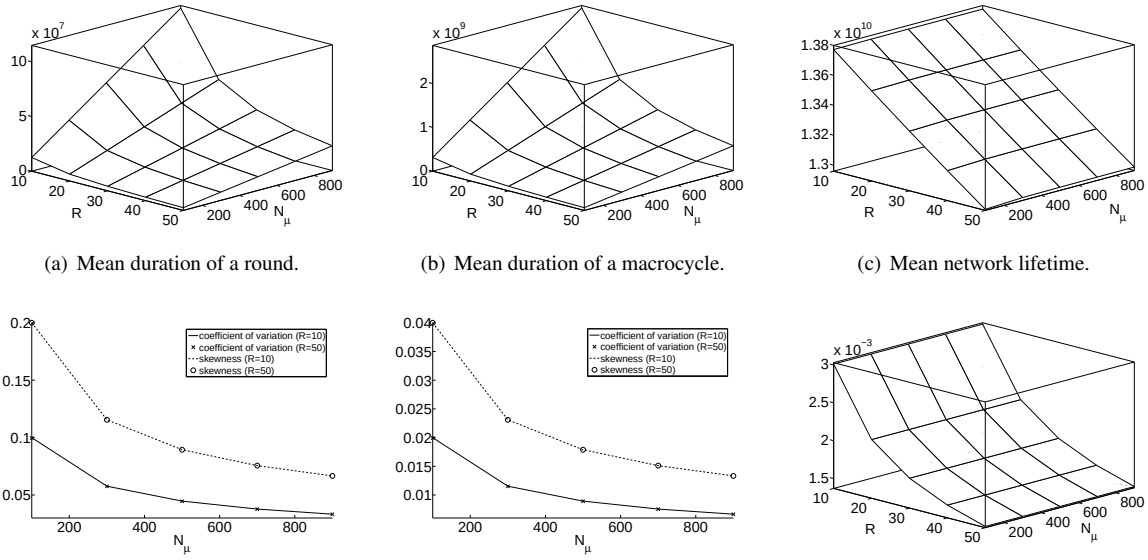

(a) Mean duration of a round. (b) Mean duration of a macrocycle. (c) Mean network lifetime.

(d) Coefficient of variation and skewness of a round. (e) Coefficient of variation and skewness of a macrocycle. (f) Coefficient of variation of lifetime.

Fig. 6. Performance vs. sensing reliability R and number of microcycles N_μ.

the mean and, consequently, higher values of coefficient of variation. Also, a macrocycle has smaller skewness than a round, as can be seen in Figs. 5(d) and 5(e), which is due to the fact that, according to the central limit theorem [7], sum of a number of iid random variables converges to a normal distribution with zero skewness. Since the network lifetime is composed of macrocycles, the same argument holds with respect to the coefficient of variation of network lifetime, shown in Fig. 5(f). Higher values of CV indicate higher variation of lifetime, which means that the network may cease to operate even though many nodes still haven't exhausted their energy supply. Lower values for the coefficient of variation are desirable as they indicate longer network lifetime and better energy efficiency.

6.2. Variable event sensing reliability and clustering period

In our second experiment, we have investigated the performance of the ALEC approach under variable event sensing reliability R and variable clustering period, controlled by the number of microcycles N_μ. the results obtained with $N_c = 16$ clusters, which means that each cluster had $n_c = N/N_c = 25$ nodes, are shown in Fig. 6.

As can be expected, values of sensing reliability affect the mean duration of a round or a macrocycle in a similar way as in the previous experiment, although the dependency is much less pronounced than in Fig. 5(a). Increasing the number of microcycles increases the mean duration for both round and macrocycle periods. As the macrocycle consists of a number of rounds, increasing the number of macrocycles translates into lower values for both coefficient of variation and skewness, as the level of rounds, Fig. 6(d), as well as at the level of macrocycles, Fig. 6(e). However, skewness of a macrocycle is smaller than that of a round which implies that macrocycles are closer to normal distribution. Since lifetime is composed of a number of macrocycles, similar argument holds for the coefficient of variation of network lifetime, shown in Fig. 6(f). When the required event sensing reliability decreases, the number of macrocycles during the network lifetime decreases, which leads to higher dispersion around the mean value and higher values of coefficient of variation.

6.3. Variable number of clusters and microcycles

We have also investigated performance of the ALEC approach under variable number of clusters N_c and

DOI: 10.1002/wcm

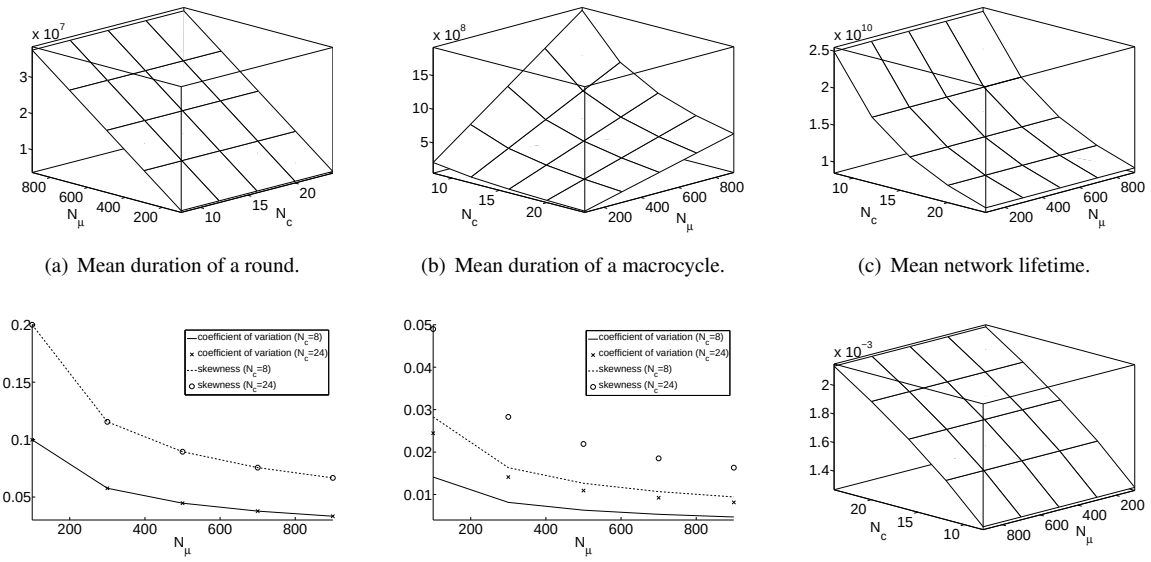

(a) Mean duration of a round. (b) Mean duration of a macrocycle. (c) Mean network lifetime.

(d) Coefficient of variation and skewness of a round. (e) Coefficient of variation and skewness of a macrocycle. (f) Coefficient of variation of lifetime.

Fig. 7. Performance vs. number of clusters N_c and number of microcycles N_μ.

variable number of microcycles N_μ, while keeping the event sensing reliability and, consequently, packet arrival rate at constant value of $R = 30$ and $r = 0.075$ packets per second per node, respectively. The results are shown in Fig. 7.

As can be seen, higher number of microcycles leads to higher mean duration of a round, Fig. 7(a). The duration of a macrocycle, being a sum of duration of a number of rounds, increases when the number of clusters decreases and/or the number of microcycles increases, as shown in Fig. 7(b). The network lifetime, on the contrary, increases when there are fewer clusters, but is rather insensitive to the number of microcycles, Fig. 7(c), due to multiple levels of summation between the two.

Coefficient of variation and skewness for a round and macrocycle are shown in Figs. 7(d) and 7(e), respectively. When the round contains fewer microcycles (below 200), coefficient of variation as well as skewness are higher, which leads to higher dispersion around the mean value. Increasing the number of microcycles, which are summed to obtain a round, results in lower dispersion around mean value for a round, and the same observation holds for a macrocycle. Again, the skewness of a macrocycle is smaller than that of a round, which means the duration of a macrocycle is closer to normal distribution. Coefficient of variation of lifetime is shown in Fig. 7(f); as can be seen, lower dispersion around the mean can be achieved by lowering the number of clusters which, in turn, results in larger number of rounds in a macrocycle.

6.4. Power consumption and delay overheads

The ALEC algorithm incurs some amount of overhead due to clustering. As mentioned before, no data can be transmitted to BS during the set-up phase, which will delay delivery of some sensing data. On the other hand, energy consumption during set-up phase does not directly contribute to data collection so it may be considered as energy overhead. Obviously, minimizing both delay and energy overhead is a primary measure of the efficiency of a clustering algorithm.

To evaluate the efficiency of the ALEC algorithm, we have also calculated the delay and energy overhead introduced by the use of ALEC algorithm; the results are shown in Fig. 8, with delay overhead shown in the diagrams in the top row and energy overhead in the diagrams in the bottom row.

Regarding the delay overhead incurred by the ALEC algorithm, results shown in Fig. 8(a) are obtained with the number of microcycles fixed at 500, those in Fig. 8(b) are obtained with the number of clusters fixed at 16, and those in Fig. 8(c) are obtained

DOI: 10.1002/wcm

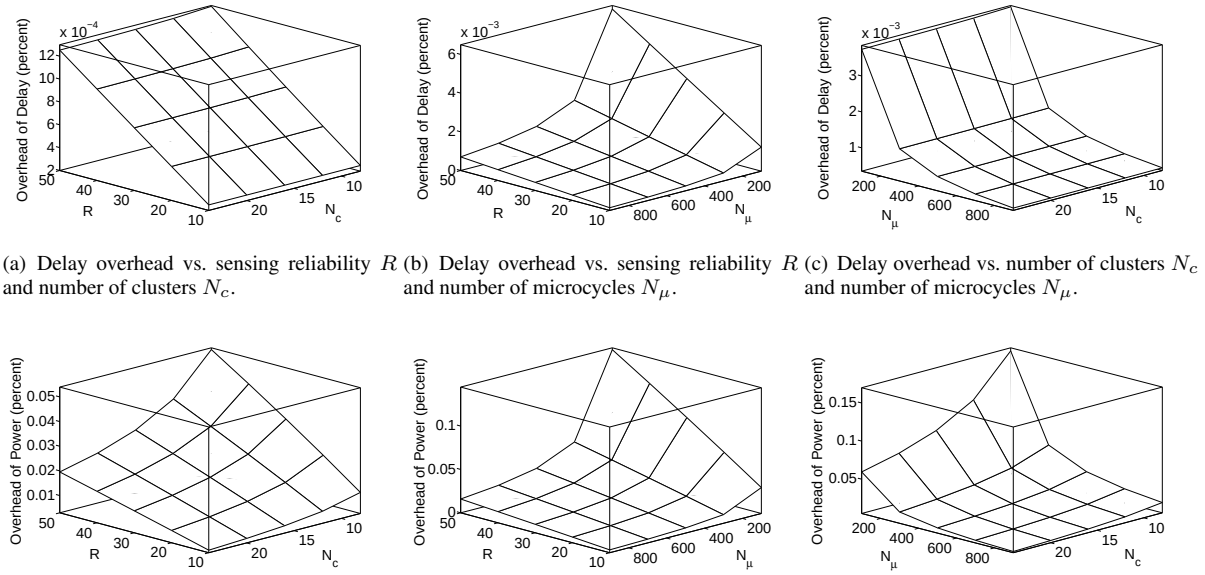

(a) Delay overhead vs. sensing reliability R and number of clusters N_c.

(b) Delay overhead vs. sensing reliability R and number of microcycles N_μ.

(c) Delay overhead vs. number of clusters N_c and number of microcycles N_μ.

(d) Power consumption overhead vs. sensing reliability R and number of clusters N_c.

(e) Power consumption overhead vs. sensing reliability R and number of microcycles N_μ.

(f) Power consumption overhead vs. number of clusters N_c and number of microcycles N_μ.

Fig. 8. Overhead (in percent) due to ALEC algorithm.

with sensing reliability fixed at 30. Overall, the delay overhead is below 0.65% in all three experiments which is rather low. As can be seen, lower values of delay overhead can be achieved by increasing the number of clusters or the number of microcycles. Delay overhead could also be decreased by lowering the event sensing reliability – provided the application allows it.

The energy overhead incurred by the ALEC algorithm is calculated as the ratio of total energy consumed by the network during the set-up phase and the total energy consumption of the network. As above, the results in Fig. 8(d) are obtained with the number of microcycles fixed at 500, those in Fig. 8(e) are obtained at the number of clusters fixed at 16, and those in Fig. 8(f) are obtained under sensing reliability fixed at 30. Overall, the energy overhead is less than 0.15% in the observed range of independent variables which is negligible. Still, energy overhead may be reduced by increasing the number of clusters and/or microcycles. It may also be reduced by lowering the event sensing reliability, as long as the application requirements allow for such a reduction.

7. Conclusion

In this paper, we have presented the Adaptive Low-Energy Clustering (ALEC) algorithm for sensor networks using sensor nodes operating in IEEE 802.15.4 slotted beacon-enabled mode. Nodes in an ALEC-operated network use random sleep to extend their lifetime. They also use clustering to improve efficiency, with the role of cluster-head taken by different nodes in random periods in order to balance the energy consumption and thus extend the useful lifetime of the network. We have used probabilistic and queuing analysis to investigate how different ALEC parameters such as the number of clusters and number of microcycles, as well as application-dictated parameters such as event sensing reliability, impact the performance of the network in particular the network lifetime and clustering overhead. Our results indicate that energy consumption overhead and delay overhead of the ALEC algorithm are not only low, but are well below the variability due to the randomness inherent to the ALEC algorithm. Moreover, low values of the coefficient of variability and skewness indicate that the node energy consumption is well balanced, which means all nodes will die at approximately the same time, thus extending the useful life of the network itself.

DOI: 10.1002/wcm

Our future work will focus on improving the ALEC algorithm by fine-tuning its parameters. We will also investigate the possibility of aggregating the sensed data in order to improve the transmission efficiency.

References

1. Chipcon CC2420 Datasheet: 2.4 GHz IEEE 802.15.4 / ZigBee-Ready RF Transceiver (Rev. B), Feb. 2012.
2. X. Bian, X. Liu, and H. Cho. Study on a cluster-chain routing protocol in wireless sensor networks. In *3rd Int. Conf. Communications and Networking in China (ChinaCom 2008)*, pp. 964–968, Aug. 2008.
3. O. Boyinbode, H. Le, A. Mbogho, M. Takizawa, and R. Poliah. A Survey on Clustering Algorithms for Wireless Sensor Networks. In *13th Int. Conf. Network-Based Information Systems (NBiS 2010)*, pp. 358–364, Sept. 2010.
4. G. Chen, F. Nocetti, J. Gonzalez, and I. Stojmenovic. Connectivity based k-hop clustering in wireless networks. In *35th Ann. Hawaii Int. Conf. System Sciences (HICSS 2002)*, pp. 2450–2459, Jan. 2002.
5. S. C. Ergen and P. Varaiya. TDMA scheduling algorithms for wireless sensor networks. *Wirel. Netw.*, 16(4):985–997, May 2010.
6. M. Ghelichi, S. Jahanbakhsh, and E. Sanaei. RCCT: Robust Clustering with Cooperative Transmission for Energy Efficient Wireless Sensor Networks. In *5th Int. Conf. Information Technology: New Generations (ITNG 2008)*, pp. 761–766, April 2008.
7. G. R. Grimmett and D. R. Stirzaker. *Probability and Random Processes*. Clarendon Press, Oxford, second edition, 1992.
8. M. Handy, M. Haase, and D. Timmermann. Low energy adaptive clustering hierarchy with deterministic cluster-head selection. In *4th Int. Workshop Mobile and Wireless Communications Networks*, pp. 368–372, 2002.
9. W. Heinzelman, A. Chandrakasan, and H. Balakrishnan. Energy-efficient communication protocol for wireless microsensor networks. In *33rd Ann. Hawaii Int. Conf. System Sciences (HICSS 2000)*, page 10, vol.2, Jan. 2000.
10. W. Heinzelman, A. Chandrakasan, and H. Balakrishnan. An application-specific protocol architecture for wireless microsensor networks. *IEEE Trans. Wireless Comm.*, 1(4):660–670, Oct. 2002.
11. J. Hong, J. Kook, S. Lee, D. Kwon, and S. Yi. T-LEACH: The method of threshold-based cluster head replacement for wireless sensor networks. *Information Systems Frontiers*, 11(5):513–521, Nov. 2009.
12. IEEE. Wireless MAC and PHY specifications for low rate WPAN. IEEE Std 802.15.4-2006 (Revision of IEEE Std 802.15.4-2003), IEEE, New York, NY, 2006.
13. N. Johansson, U. Körner, and L. Tassiulas. A distributed scheduling algorithm for a Bluetooth scatternet. In *International Teletraffic Congress*, 2001.
14. J. Kim, J. Lee, and K. Rim. 3DE: selective cluster head selection scheme for energy efficiency in wireless sensor networks. In *Proc. 2nd Int. Conf. Pervasive Technologies Related to Assistive Environments (PETRA'09)*, pp 33:1–33:7, New York, NY, USA, 2009. ACM.
15. X. Li, G. Fletcher, A. Nayak, and I. Stojmenovic. Randomized carrier-based sensor relocation in wireless sensor and robot networks. *Ad Hoc Networks*, 2012.
16. M. Maimour, H. Zeghilet, and F. Lepage. Cluster-based Routing Protocols for Energy-Efficiency in Wireless Sensor Networks. In *Sustainable Wireless Sensor Networks*, pp. 167–188. INTECH, Dec. 2010. 22 pages.
17. J. Mišić, S. Shafi, and V. B. Mišić. Cross-layer activity management in a 802.15.4 sensor network. *IEEE Communications Magazine*, 44(1):131–136, Jan. 2006.
18. J. Mišić. Traffic and energy consumption of an IEEE 802.15.4 network in the presence of authenticated, ECC Diffie-Hellman ephemeral key exchange. *Computer Networks*, 52(11):2227–2236, 2008.
19. J. Mišić. Cost of secure sensing in IEEE 802.15.4 networks. *IEEE Trans. Wireless Comm.*, 8(5):2494–2504, may 2009.
20. S. Naeimi, H. Ghafghazi, C.-O. Chow, and H. Ishii. A Survey on the Taxonomy of Cluster-Based Routing Protocols for Homogeneous Wireless Sensor Networks. *Sensors*, 12(6):7350–7409, 2012.
21. M. Noori and M. Ardakani. A Probabilistic Lifetime Analysis for Clustered Wireless Sensor Networks. In *Wireless Communications and Networking Conference, 2008. WCNC 2008. IEEE*, pp. 2373–2378, April 2008.
22. T. Rappaport. *Wireless communications: Principles & Practice*. Prentice Hall, Upper Saddle River, NJ 07458, 1996.
23. Y. Sankarasubramaniam, Ö. B. Akan, and I. F. Akyildiz. ESRT: event-to-sink reliable transport in wireless sensor networks. In *Proc. 4th ACM MobiHoc*, pp. 177–188, Annapolis, MD, June 2003.
24. R. Srivathsan, S. Siddharth, R. Muthuregunathan, R. Gunasekaran, and V. Uthariaraj. Enhanced Genetic algorithm for solving broadcast scheduling problem in TDMA based wireless networks. In *Second Int. Conf. Communication Systems and Networks (COMSNETS 2010)*, pp. 1–10, Jan. 2010.
25. I. Stojmenović, editor. *Handbook of Sensor Networks: Algorithms and Architectures*. John Wiley & Sons, 2005.
26. I. Stojmenovic, M. Seddigh, and J. Zunic. Internal nodes based broadcasting in wireless networks. In *34th Ann. Hawaii Int. Conf. System Sciences (HICSS 2001)*, page 10, Jan. 2001.
27. I. Stojmenovic, M. Seddigh, and J. Zunic. Dominating Sets and Neighbor Elimination-Based Broadcasting Algorithms in Wireless Networks. *IEEE Trans. Parallel Distrib. Syst.*, 13(1):14–25, Jan. 2002.
28. H. Su and X. Zhang. Energy-Efficient Clustering System Model and Reconfiguration Schemes for Wireless Sensor Networks. In *40th Ann. Conf. Information Sciences and Systems*, pp. 99–104, March 2006.
29. H. Takagi. *Queueing Analysis*, volume 1: Vacation and Priority Systems. North-Holland, Amsterdam, The Netherlands, 1991.
30. G. Thonet, P. Allard-Jacquin, and P. Colle. ZigBee - WiFi Coexistence. Technical report, Schneider Electric, Innovation Department 37 Quai Paul Louis Merlin 38000 Grenoble, France, April 2008.
31. O. Younis and S. Fahmy. HEED: a hybrid, energy-efficient, distributed clustering approach for ad hoc sensor networks. *IEEE Trans. Mobile Computing*, 3(4):366–379, 2004.

DOI: 10.1002/wcm